Available online at www.sciencedirect.com

SCIENCE DIRECT

Biochimica et Biophysica Acta 1706 (2005) 250–261

BIOCHIMICA ET BIOPHYSICA ACTA
BBA

http://www.elsevier.com/locate/bba

Methylviologen and dibromothymoquinone treatments of pea leaves reveal the role of photosystem I in the Chl *a* fluorescence rise OJIP

Gert Schansker*, Szilvia Z. Tóth, Reto J. Strasser

Bioenergetics Laboratory, University of Geneva, Chemin des Embrouchis 10, CH-1254 Jussy, Geneva, Switzerland

Received 5 August 2004; received in revised form 16 November 2004; accepted 18 November 2004
Available online 2 December 2004

Abstract

The effects of dibromothymoquinone (DBMIB) and methylviologen (MV) on the Chl *a* fluorescence induction transient (OJIP) were studied in vivo. Simultaneously measured 820-nm transmission kinetics were used to monitor electron flow through photosystem I (PSI). DBMIB inhibits the reoxidation of plastoquinol by binding to the cytochrome b_6/f complex. MV accepts electrons from the FeS clusters of PSI and it allows electrons to bypass the block that is transiently imposed by ferredoxin-$NADP^+$-reductase (FNR) (inactive in dark-adapted leaves). We show that the IP phase of the OJIP transient disappears in the presence of DBMIB without affecting F_m. MV suppresses the IP phase by lowering the P level compared to untreated leaves. These observations indicate that PSI activity plays an important role in the kinetics of the OJIP transient. Two requirements for the IP phase are electron transfer beyond the cytochrome b_6/f complex (blocked by DBMIB) and a transient block at the acceptor side of PSI (bypassed by MV). It is also observed that in leaves, just like in thylakoid membranes, DBMIB can bypass its own block at the cytochrome b_6/f complex and donate electrons directly to PC^+ and $P700^+$ with a donation time τ of 4.3 s. Further, alternative explanations of the IP phase that have been proposed in the literature are discussed.

Keywords: Chl *a* fluorescence; OJIP-transient; 820-nm transmission; DBMIB; Methylviologen; *Pisum sativum*

1. Introduction

The Chl *a* fluorescence induction transient (OJIP) has been studied extensively (for recent reviews, see Refs. [1–4]). In the last few years several mutually exclusive hypotheses have been put forward to explain the second and third kinetic phases of the initial fluorescence rise (JI and IP). Here, we will concentrate on the physiological processes underlying the IP phase for which at least eight hypotheses have been presented during the last 45 years. Initially, it was thought that the reduction of an electron acceptor at the acceptor side of photosystem I (PSI) was responsible for the IP phase [5–8]. Schreiber and Vidaver [9] proposed energy redistribution between PSII and PSI. The observations of Vernotte et al. [10] have been interpreted to mean that the IP phase can be explained by removal of plastoquinone (PQ) pool quenching as a consequence of reduction of the PQ pool (e.g., Refs. [11,12]). The IP phase has also been thought to represent variable PSI fluorescence [13,14], an effect of the electric field [15] or the last step in the reduction of the acceptor side of PSII [16]. Two more interpretations that have been put forward are recombinational fluorescence (with respect to the whole thermal phase of the fluorescence induction curve) [17] and slowly closing stromal PSII reaction centers [14].

Some of these interpretations may have to do with the fact that they were based on experiments with thylakoid

Abbreviations: Chl, chlorophyll; DBMIB, dibromothymoquinone, 2,5-dibromo-3-methyl-6-isopropyl-*p*-benzoquinone; DCMU, 3-(3,4-dichlorophenyl)-1,1′-dimethylurea; F_o and F_m, fluorescence intensity measured when all photosystem II reaction centers are open or closed, respectively; FNR, ferredoxin-$NADP^+$-reductase; I, photocurrent, a measure for the transmitted light; LED, light emitting diode; MV, methylviologen, 1,1′-dimethyl-4,4′-bipyridinium-dichloride; OJIP-curve, fluorescence induction transient defined by the names of its intermediate steps, O level, fluorescence level at 20 μs, J level, fluorescence plateau at ~2 ms, I level, fluorescence plateau at ~30 ms and P level, the maximum fluorescence level; P680 and P700, reaction center pigments of photosystem II and I, respectively; PC, plastocyanin; Q_A, primary quinone electron acceptor of photosystem II

* Corresponding author. Tel.: +41 22 759 9940; fax: +41 22 759 9945.
E-mail address: Gert.Schansker@bioen.unige.ch (G. Schansker).

0005-2728/$ - see front matter © 2004 Elsevier B.V. All rights reserved.
doi:10.1016/j.bbabio.2004.11.006

membranes. During the isolation of thylakoid membranes, ferredoxin on the acceptor side of PSI is lost and this changes the Chl *a* fluorescence rise. For example, no clear I-step is observed in thylakoid membranes [18–21].

Here, we have studied the effects of dibromothymoquinone (DBMIB) and methylviologen (MV) in vivo using Chl *a* fluorescence and transmission measurements at 820 nm. Both DBMIB and MV strongly affect the IP phase of the fluorescence induction transient, each for its own reason. Our results support the original hypothesis [5–8] that the IP phase is related to electron transfer through PSI and the induction of a traffic jam of electrons caused by a transient block at the acceptor side of PSI (inactive ferredoxin-$NADP^+$-reductase (FNR)).

2. Materials and methods

2.1. Plant material

For the measurements, mature leaves of 2–3-week-old pea plants (*Pisum sativum* L. cv. Ambassador) were used. Plants were grown in a greenhouse where the temperature was 20–25 °C during the day and 14–16 °C at night.

2.2. MV treatment

For the MV treatments, a 200 μM MV (1,1′ -dimethyl-4,4′ -bipyridinium-dichloride, Fluka) solution was applied to both sides of the leaf with a fine brush. The leaves were not detached and the plants were kept overnight in complete darkness before the measurements were made. Stirring clipped leaves for 12 min in 200 μM MV as done for the DBMIB treatment (see below) gave very similar results (not shown).

MV+DCMU treatment: Pea leaves were submerged into a solution containing 200 μM MV, 170 μM DCMU and 1% ethanol. Leaves were not detached and they were treated overnight in complete darkness.

2.3. DBMIB treatment

Overnight incubation of undetached leaves in a DBMIB solution was not effective. Instead, leaves with clipped edges to allow a better uptake were stirred for 12 min in a solution of 200 μM DBMIB (2,5-dibromo-3-methyl-6-isopropyl-*p*-benzoquinone, SIGMA) containing 1% of ethanol. The leaves were stored in the DBMIB solution until use. Leaves treated in the same way, but in the absence of DBMIB, were used as controls.

DBMIB+DCMU treatment: First, leaves were treated with DCMU (170 μM DCMU, 1% ethanol). Leaves were not detached and they were treated overnight in complete darkness. Subsequently, they were treated with DBMIB, as described above.

2.4. Measuring equipment

Chl *a* fluorescence emission was measured by a Handy PEA (Handy PEA-Plant Efficiency Analyser, Hansatech Instruments, King's Lynn, Norfolk, UK). Leaves were dark-adapted for 30 min before they were measured. Illumination (unless stated otherwise) consisted of a 1-s pulse of continuous red light (650-nm peak wavelength, 3000 μmol photons m^{-2} s^{-1} maximum light intensity) provided by an array of three light-emitting diodes (LEDs) focused on a leaf area with a diameter of 5 mm.

Transmission changes at 820 nm and Chl *a* fluorescence were recorded simultaneously using a dual channel PEA Senior instrument (Hansatech Instruments). The first reliable measuring point for fluorescence change was at 20 μs whereas the first measuring point for transmission change was at 400 μs. The time constant used for the transmission measurements was 100 μs. The light intensity used for all experiments was 1800 μmol photons m^{-2} s^{-1}. The light was produced by four 650-nm LEDs. The far-red light source was a QDDH73520 LED (Quantum Devices Inc.) filtered at 720±5 nm. The modulated (33.3 kHz) far-red measuring light was provided by an OD820 LED (Opto Diode Corp.) filtered at 830±20 nm. Executing commands like turning on and off the LEDs took about 250 μs. Turning on the red light and starting the measurement were synchronized commands. For the far-red light there was a delay of 250 μs between turning on the far-red light and the start of the measurement. Each measurement consisted of three parts. First, the transmission was measured without amplification and offset to obtain a value for total transmission (I_0). Subsequently, the transmission was measured with a gain of 50 to obtain a value for the transmission at t=0. This was followed by kinetic measurements.

3. Results

3.1. Chl a fluorescence rise

DBMIB is an artificial quinone introduced in 1970 by Trebst et al. [22] and Böhme et al. [23] as an inhibitor of photosynthetic electron transport and an antagonist of PQ. It was shown that cyt b_6/f can accept only one electron from DBMIB. As a semiquinone it remains tightly bound to the cyt b_6/f complex preventing in this way the reoxidation of other PQH_2 molecules by cyt b_6/f [24]. The DBMIB concentration used in this study inhibits the cyt b_6/f complex but it also has a limited effect on the Q_B site. In Fig. 1A several fluorescence induction curves in the presence and absence of DBMIB measured at different light intensities are shown. The main effect of DBMIB is to make the IP phase disappear, which means that under saturating light conditions the I level approaches the maximum fluorescence level. On the other hand, the F_m level is not affected by the treatment. It can also be observed

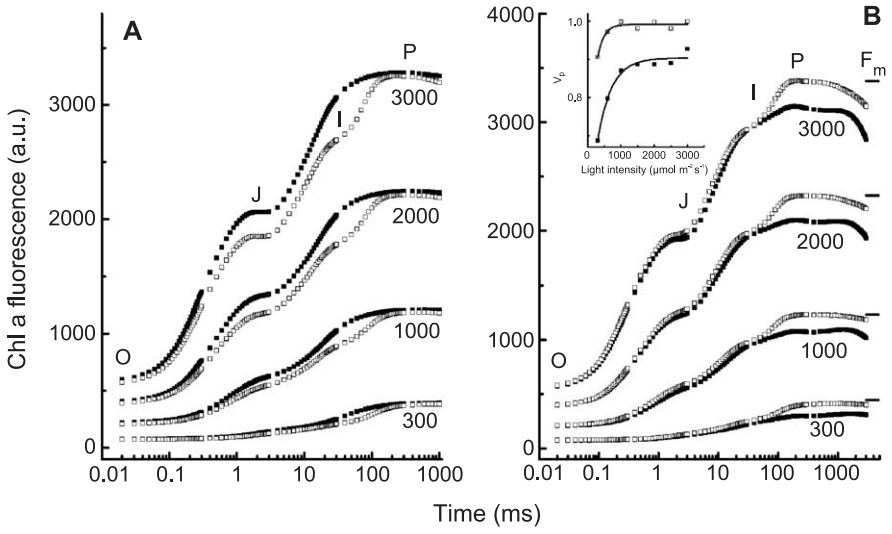

Fig. 1. Effect of DBMIB (panel A) and MV (panel B) on the Chl *a* fluorescence induction curve of pea leaves. The fluorescence induction transients (averages of about 20 measurements each) are shown as measured. Closed symbols are the treated and open symbols the control leaves. Control leaves were treated in the same way as the DBMIB- or MV-treated leaves, respectively. The light intensity (in μmol photons m^{-2} s^{-1}) at which the induction curves were recorded is indicated in the panels. The inset of panel B shows the relative variable fluorescence at the P level (V_P) calculated as $((F_m/F_o-1)_{\times \mu mol\ m^{-2}\ s^{-1}}/(F_m/F_o-1)_{3000\ \mu mol\ m^{-2}\ s^{-1}})$ as a function of the light intensity. It was assumed that the ratio F_o/F_m is independent of the light intensity and the F_m values calculated on this basis are indicated in panel B. See Materials and methods for further details.

that full inhibition of electron transport by DBMIB induces a higher J level (~5% of F_v) and a slightly higher F_o level (~4% of F_o) (Fig. 1A). The effect of DBMIB on the shape of the fluorescence induction curve can be observed at all measured light intensities.

Several authors have written about the effect of MV on the fluorescence induction curve. Munday and Govindjee [6] observed that infiltration of *Chlorella pyrenoidosa* cells with MV strongly reduced the amplitude of the IP phase, but had little effect on the OI phase. Neubauer and Schreiber [11] observed that high light-illumination of MV-treated chloroplasts suppressed the IP phase and lowered the F_m level. Harbinson and Hedley [25] observed a lower F_m/F_o ratio in MV-treated leaves. Fig. 1B shows that MV suppresses selectively the IP phase independent of the light intensity. No effects of the presence of MV on either the F_o or J level are observed (see also Fig. 5). Our data (see inset of Fig. 1B) do not exclude the possibility that a further increase of the light intensity would reduce the difference between F_m (control) and F_m (MV) and thus lead to a more complete reduction of Q_A. The F_m level measured after a double infiltration of leaves with DCMU and MV is almost identical to the F_m level measured in control leaves (not shown). This observation and the absence of an effect on the O-J-I rise kinetics indicate that treatment with MV did not cause photo-oxidative damage.

3.2. Dark-adaptation kinetics of the Chl a fluorescence rise

In Fig. 2 the dark-adaptation kinetics of the Chl *a* fluorescence induction transient after a 0.7-s red pre-pulse of 3000 μmol m^{-2} s^{-1} is shown for untreated control leaves (Fig. 2A), in the presence of DBMIB (Fig. 2B) or MV (Fig. 2C). Comparing the dark-adaptation kinetics of control leaves with DBMIB-treated leaves, several differences are observed. The dip between the J level and F_m that is so prominent in control leaves at short time intervals between the pulses is missing in DBMIB-treated leaves. Long ago, it was demonstrated for leaves kept under anaerobic conditions that this dip is related to a transient oxidation of the PQ pool (and Q_A^-) by PSI (e.g., Refs. [5,7]). The DBMIB measurements confirm this interpretation. The most striking effect of MV (Fig. 2C) is that in its presence the dark-adaptation kinetics of the Chl *a* fluorescence induction curves are very fast. The dark-adaptation kinetics in the IP-region (Fig. 2C) also indicate that the IP phase is strongly but not completely suppressed by MV.

In Fig. 3 the dark-adaptation kinetics of the O and J levels derived from transients like the ones shown in Fig. 2 are presented. In the case of the DBMIB treatment, an extra control, leaves treated with 1% ethanol (which was used to dissolve the DBMIB), is presented. Panels A and B of Fig. 3 indicate that ethanol has a small effect on the reoxidation kinetics of the electron transport chain. The clearest difference observed in panel B is an increase of the J level that might indicate a slight perturbation of the Q_B site by the presence of the ethanol.

For the O level of the control (panel A) biphasic kinetics with decay times of 0.6 and 40 s are observed, whereas for the J level of the control (panel B) a decay time of 71 s is determined. Looking at the effect of the DBMIB on the dark-adaptation kinetics, we observe that the slowest phase of the dark-adaptation kinetics of the O level has a much smaller amplitude in the presence of DBMIB (see arrow in panel A) and for the J level the occurrence of a second

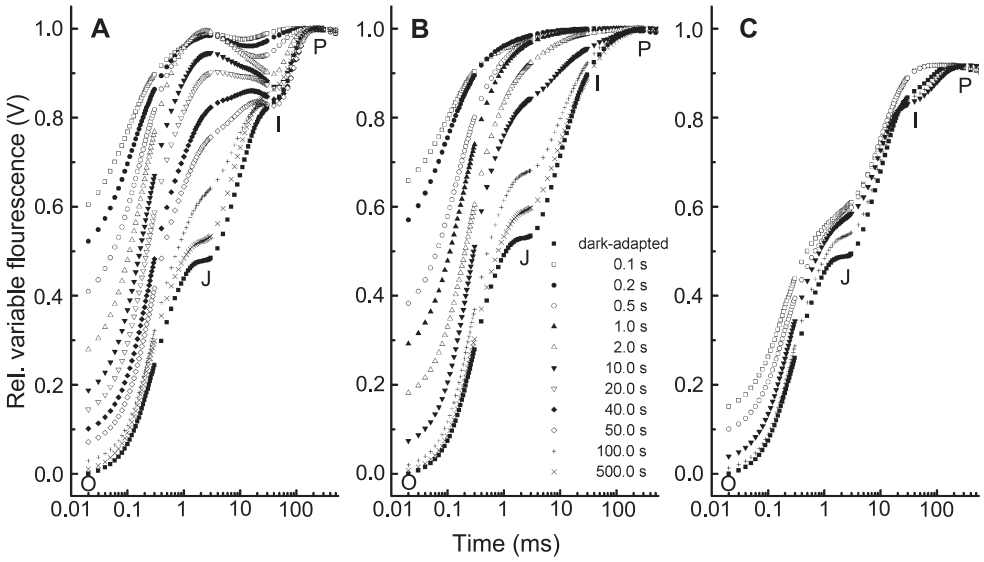

Fig. 2. Dark-adaptation kinetics of the Chl *a* fluorescence induction curve following a saturating pulse of red light in control leaves (A), DBMIB-treated leaves (B) and MV-treated leaves (C). The fluorescence transients were double normalized between the F_o and F_m levels of the first pulse and in the case of the MV-treated leaves the calculated F_m (see Fig. 1B), instead of the measured P level, was used for the normalization. The dark-interval time between the first and the second pulse is indicated in panel B for each symbol. For reasons of clarity, not all time intervals are shown for each treatment. Each transient represents the average of about 20 measurements.

phase with a decay time of 3.9 s and representing about a third of the total amplitude is observed (indicated by an arrow in panel B).

The dark-adaptation kinetics of the O (panel C) and J levels (panel D) in the presence of MV are much faster than in its absence; after 100 ms of dark-adaptation, the O level in the presence of MV is only a third of that in its absence. This effect is also observed for the J level (panel D). Already, during the first 100 ms after the end of the first pulse the value for the J level has decreased strongly, whereas in control leaves no change is observed during the first 10 s of dark-adaptation. This reflects an almost complete reoxidation of the PQ pool (see also below). In a way, it is remarkable that for the O level (panel C), the dark-adaptation kinetics of the control and MV-treated samples are similar, despite the availability of oxidized PQ molecules: approximately a third of the O level amplitude dark-adapts like in control samples (Fig. 3C).

3.3. Effects of MV and DBMIB on the 820-nm transmission level during red and far-red illuminations

In Fig. 4, the effects on the 820-nm transmission level of a red (0.7 s, 1800 μmol m^{-2} s^{-1})–far-red (15 s, 200 μmol m^{-2} s^{-1})–red (2 s, 1800 μmol m^{-2} s^{-1}) light sequence inducing a sequential reduction, oxidation and reduction of the electron transport chain in control leaves are shown. By filling, emptying and filling again the electron transport chain, the oxidation and reduction properties of the chain are made visible. For the control leaves we observe that the red light induces an initial oxidation of PC and P700 followed by a full reduction. In both the DBMIB- and MV-treated leaves, this re-reduction phase is missing. Instead, a further oxidation occurs, although in the presence of MV no full oxidation of PC and P700 is achieved (compare the lowest transmission level of the MV trace with that of the DBMIB trace). DBMIB effectively prevents PSII electrons from reaching PC and P700, and MV accepts electrons from the electron transport chain at almost the same rate as PSII is pumping them into the chain. The subsequent FR pulse oxidizes PC, P700 and Fd nearly completely under all three conditions. In the DBMIB-treated leaves we observe only a small transient increase in the 820-nm transmission value. The fact that the transmission level is similar at the beginning and at the end of the far-red light pulse indicates that PC, P700 and Fd were almost completely oxidized by the preceding red light pulse. In the presence of MV the behaviour is quite different. The transmission level is low at the beginning of the measurement, increases as electrons from the (partially) reduced PQ pool reduce PC^+ and $P700^+$ but subsequently return to a low level as the far-red light oxidizes the whole electron transport chain. Making the same measurement in the absence of (far-red) light, the same increase of the transmission level is observed but in this case the re-reduction phase continues and is completed within 100 ms (not shown). Finally, the second red light pulse re-reduces the electron transport chain in the control leaves, whereas in the DBMIB-treated leaves PC and P700 were in the oxidized state and remained oxidized. In the MV-treated leaves a small increase of the transmission level is observed in the red light. The transmission level returns to the ‘steady state’ level observed at the end of the first red pulse.

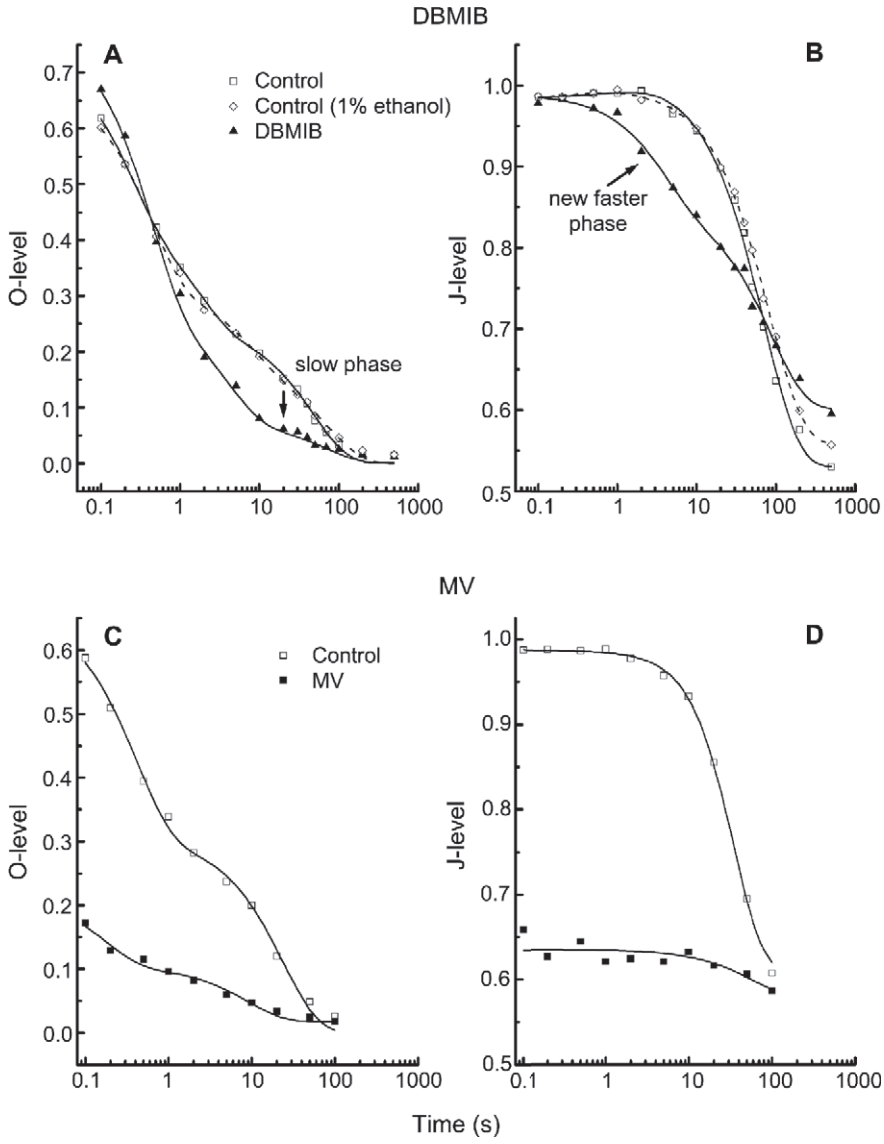

Fig. 3. Dark-adaptation kinetics of the O and J levels (as a fraction of F_v) in the presence or absence of DBMIB (panels A and B) and MV (panels C and D), respectively. The data points were obtained from measurements like the ones shown in Fig. 2. The kinetics was fitted with one to three exponential functions. Special features are indicated with an arrow. Note that the starting points of the *y*-axes are different for the different panels. In panels A and B leaves treated with either water or water containing 1% ethanol represent the controls. Each point represents the average of 20 measurements.

3.4. MV and PQ-pool reduction

Schmidt-Mende and Witt [26] measured the redox state of the PQ pool (absorbance at 254 nm) in the presence of benzylviologen (BV) in spinach chloroplasts. BV is a molecule with properties similar to those of MV. The authors observed that the PQ pool was reduced by illumination, but subsequently, half of the reduced PQ molecules were reoxidized again (within 100 ms) in darkness. The measurements of Schmidt-Mende and Witt also indicated that under their conditions the presence of BV did not decrease the absorbance change at 254 nm in the light. They assumed that in darkness electrons flow from the reduced PQ pool to oxidized P700 and they postulated plastocyanin as another potential electron acceptor in the presence of BV. We cannot measure the redox state of the PQ pool directly but, on the other hand, our data clearly show that in leaves, in the presence of MV, P700 and PC are mainly oxidized in the light (Fig. 4, left panel). We also observed that PC^+ and $P700^+$ are re-reduced in the dark within 100 ms (not shown, but see also Fig. 4, middle panel). It was, however, an open question if in the presence of MV the whole PQ pool became reduced in the light. To answer this question, we analysed the 820-nm transmission kinetics during a far-red pulse. Fig. 4 (middle panel) (also see Fig. 7) provides examples of this type of transient. The area above the fluorescence induction curve (complementary area) provides information on the number of electrons that have to be transferred before full reduction of Q_A is achieved. The area under-

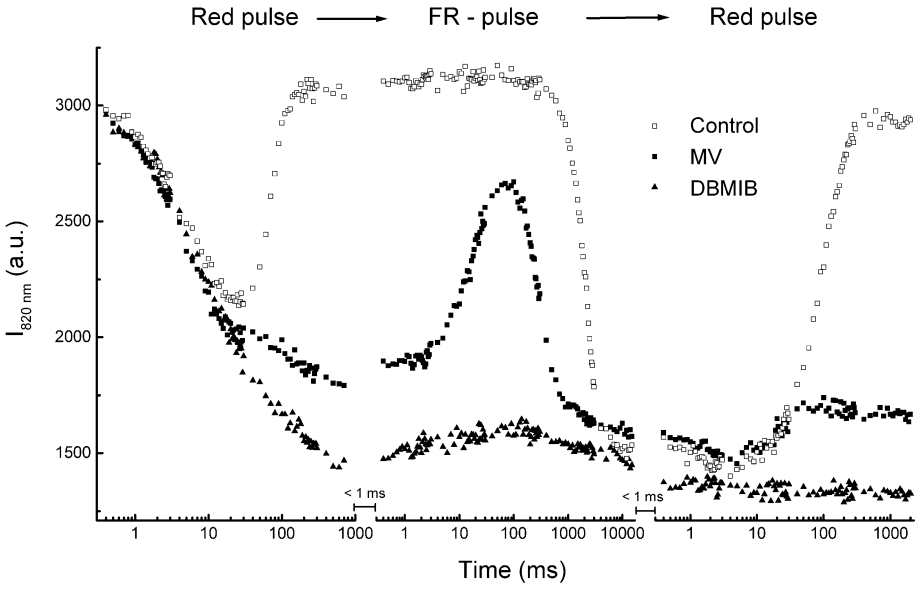

Fig. 4. Leaves were exposed to a sequence of red (2 s)–far-red (15 s)–red (2 s) light (inducing a sequential reduction, oxidation and reduction of the electron transport chain) to demonstrate the effects of DBMIB and MV on electron flow through the photosynthetic electron transport chain. The red light intensity was 1800 and the far-red light intensity 200 μmol photons m^{-2} s^{-1}. The *x*-axes provide precise information on the length and spacing of the three light pulses.

neath an 820-nm transient, as shown later in Fig. 7 (limited at the bottom side by the minimum measured transmission level), gives in a similar way information on the number of electrons that have to be removed from the electron transport chain to achieve full oxidation. After reduction of the electron transport chain by a saturating red pulse, this area increases in size: more electrons have to be removed before the electron transport chain is oxidized. The ratio between the area before and after a saturating pulse gives a measure for the redox state of the PQ pool. For control leaves the ratio between the area before a saturating red pulse and 100 ms after the pulse (calculated as $(A_{after}-A_{before})/A_{before}$) was 6, whereas for MV-treated leaves this ratio was 0.6. (It has to be noted that a far-red pre-pulse was given to control leaves 60 s before the start of the actual measurement to minimize the influx of stromal electrons [27].) The 10-fold difference in the ratio indicates that 100 ms after a saturating pulse the PQ pool is much more reduced in the control leaves than in the MV-treated leaves. A small part of this difference can be ascribed to the ~4 electrons donated by the PQ pool for the re-reduction of PC^+ and $P700^+$ during the first 100 ms after the pulse (see above). Oja et al. [28] calculated for several plant species that the control area represents three to four electrons. The PQ pool together with Q_A would then represent six times as many electrons (~20 electron equivalents). Therefore, the low area ratio observed in the presence of MV (0.6) indicates that the PQ pool remains largely oxidized in MV-treated leaves.

A relationship between the redox state of the PQ pool and the J level has been suggested before [19,27]. The fast dark-adaptation of the J level in the presence of MV may therefore be explained by the almost completely oxidized PQ pool that is observed 100 ms after the saturating red pulse (Figs. 2 and 3).

3.5. Light intensity dependence of the fluorescence induction curves

In Fig. 5 the light intensity dependence of the J and I levels is shown for control, DBMIB- and MV-treated leaves. To correct for the effect of the light intensity on the measured fluorescence levels, all data were divided by their F_o value (dividing by the respective light intensities gives very similar results). The light intensity dependence was approximated with a single exponential fit. For the DBMIB treatment (Fig. 5A) it is observed that the J and I levels saturate slightly faster than the J and I levels of the control leaves (about 25% more light is needed to half saturate the J and I levels of the control leaves). The faster saturation of the I level can easily be explained by the block of electron transfer towards PSI. A similar effect for the J level may have to do with the fact that DBMIB is a less efficient electron acceptor for PSII (see Discussion). The presence of ethanol lowers both the maximum J and I levels somewhat (~5.2% and ~3.3% of F_v, respectively) (see Fig. 5). For MV-treated leaves light intensity dependencies of the J and I levels very similar to those for control leaves are observed. This makes it very clear that a change of the electron transport activity on the acceptor side of PSI (as induced by MV) has very little effect on the J and I levels of the Chl *a* fluorescence induction curve. It may be noted that for the DBMIB-treated leaves the definition of an I level ($F_{30\ ms}$=I) may not have a physiological basis, but for a comparison of the light saturation properties of treatment and control, it is quite useful.

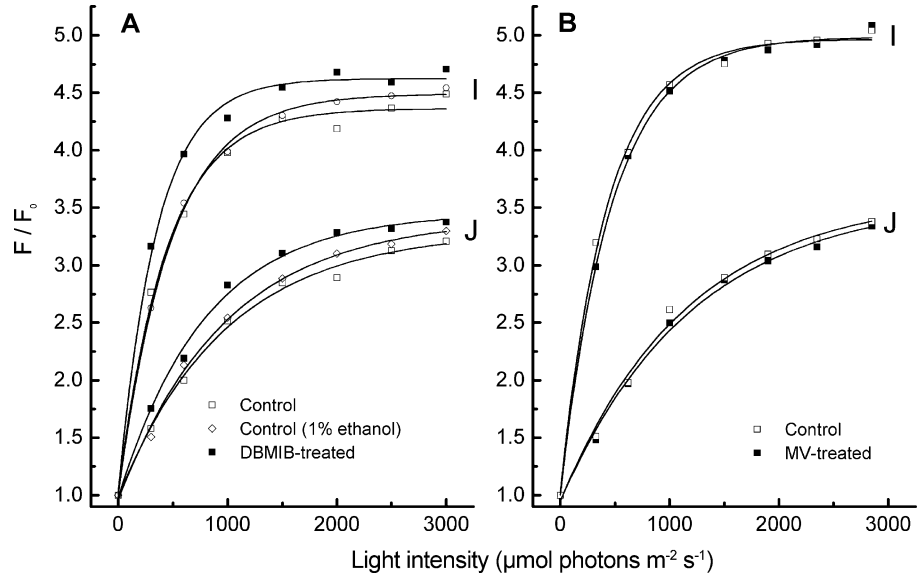

Fig. 5. Light intensity dependence of the J and I levels of the Chl *a* fluorescence induction curves of leaves treated with DBMIB (panel A) and MV (panel B). The curves were corrected for the light intensity by a division by F_o. Multiplying the curves by 1/(fraction of the maximum light intensity) gave the same result. In panel A data derived from leaves treated with either water or water containing 1% ethanol represent the controls. The light intensity dependencies were approximated by a single exponential function. Each point represents the average of about 20 measurements.

3.6. Re-reduction kinetics of PC$^+$ and P700$^+$ in darkness following a far-red pre-pulse

In Fig. 6 the re-reduction kinetics in darkness of PC$^+$ and P700$^+$ after a 15-s 200 µmol m^{-2} s^{-1} far-red pre-pulse are shown for DBMIB, MV and control leaves. For the DBMIB-treated leaves, it is observed that despite the block of the cyt b_6/f complex, the re-reduction kinetics are fast. We also observed that the re-reduction kinetics are strongly dependent on the DBMIB accumulated in the chloroplast. This is demonstrated in Fig. 6B. The measurements suggest that in leaves that are not completely inhibited two phases are observed: a phase with a decay time τ~1–1.5 s, similar to the medium phase observed in control leaves (Table 1), and a phase with a decay time τ~4–4.5 s (data not shown). Complete inhibition of the cyt b_6/f complex seems to eliminate the faster re-reduction phase and only one decay phase with a τ~4.3 s, as given in Table 1, is left. A further increase of the DBMIB concentration leads to faster re-reduction kinetics of PC$^+$ and P700$^+$ as shown in Fig. 6B

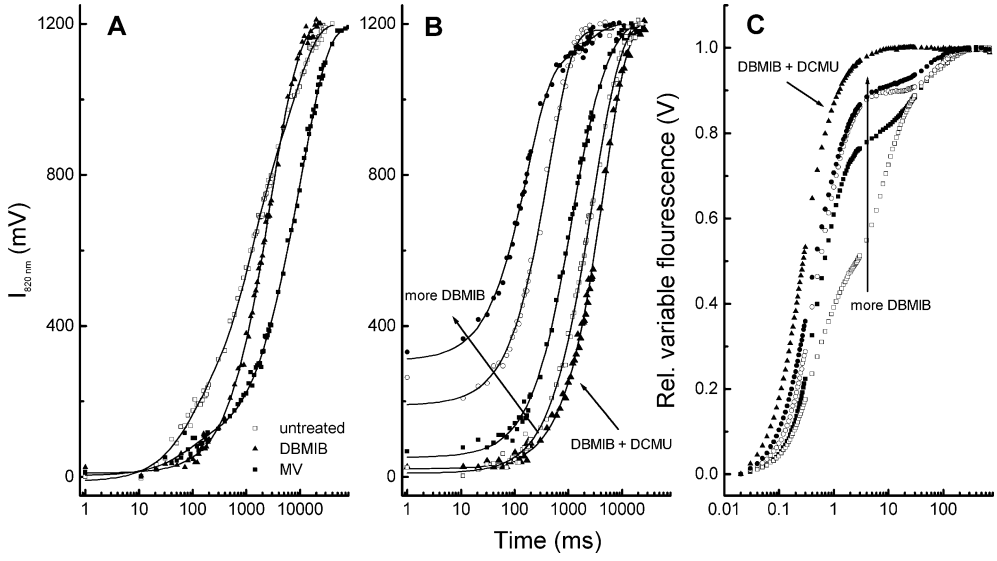

Fig. 6. Re-reduction kinetics of PC$^+$ and P700$^+$ measured at 820 nm following a 10-s far-red light pulse (200 µmol photons m^{-2} s^{-1}) in the presence or absence of either DBMIB or MV. The effects of longer incubation times with DBMIB (= higher uptake) and a double infiltration of DBMIB and DCMU are demonstrated both on the re-reduction kinetics measured at 820 nm (panel B) and the Chl *a* fluorescence induction transient (panel C). The direction of the concentration effect is indicated by an arrow. For the re-reduction kinetics each measurement was repeated three to four times on the same leaf to obtain a good signal-to-noise ratio.

(see arrow). The accumulation of DBMIB in the leaf was increased by increasing the incubation time. At the same time, the increase of the DBMIB concentration in the chloroplast leads to a lowering of the total re-reduction amplitude of the 820-nm signal (Fig. 6B), the fluorescence amplitude (not shown) and an increase of the J level (Fig. 6C). For thylakoid membranes it has been observed that addition of DBMIB in the presence of DCMU leads to a re-reduction of $P700^+$ with a halftime of 10–15 s [29]. This is considerably slower than the 4.3-s decay time observed here, but this could be due to the effect of DCMU on the redox state of the PQ pool. The effect of the redox state of the DBMIB on the re-reduction kinetics of PC^+ and $P700^+$ was assessed by treating DCMU-inhibited leaves with DBMIB. In leaves, the additional presence of DCMU causes a very limited slowdown of the re-reduction kinetics (Fig. 6B and Table 1).

In contrast, in the presence of MV the re-reduction kinetics are severalfold slower than in either the presence of DBMIB or the control. Comparing the re-reduction kinetics of control leaves with those of MV-treated leaves, a strong slowdown of the medium and slow phases is observed (Table 1 and Fig. 6A). The decay time of the fast phase is not affected by the treatment. Comparing the amplitudes of the various phases, we observe that the amplitudes of the fast and medium phases are smaller, whereas the amplitude of the slow phase is not affected (not shown). In the presence of MV and DCMU, no further slowdown of the re-reduction kinetics is observed but the fast and the medium phases are eliminated (Table 1).

3.7. Far-red light-induced transmission changes in dark-adapted leaves

The deviation from a nearly monophasic decrease of the 820-nm transmission during a far-red pulse provides information on the extent of non-photochemical reduction of the PQ pool [27]. In Fig. 7, the effect of a far-red pulse on the 820-nm transmission kinetics of dark-adapted leaves in the presence of various inhibitors/effectors is shown. For control leaves the typical transient increase of the 820-nm transmission peaking at 1.5–2 s is observed [27]. In the presence of DCMU the effect is still observed, though the kinetics are modified. In contrast, in the presence of MV, MV+DCMU (double infiltration) and DBMIB, the kinetics are seemingly monophasic and it can also be observed that the transmission decrease in the 10–200-ms range in these leaves is faster than in control leaves. The figure also shows that DCMU does not affect the kinetics that are observed in the presence of MV.

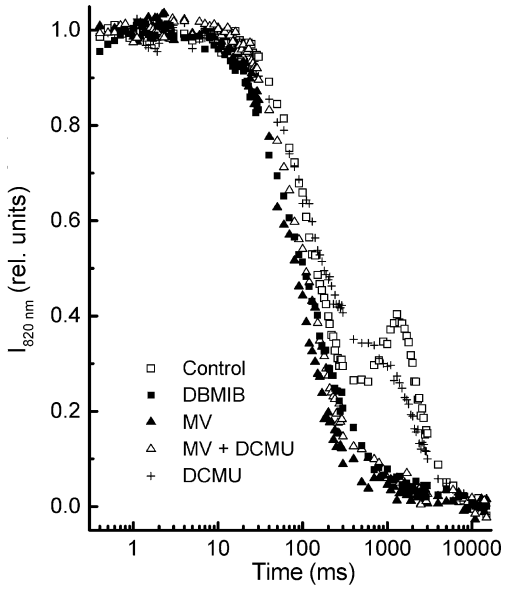

Fig. 7. Far-red light (200 μmol photons m^{-2} s^{-1})-induced oxidation kinetics of PC and P700 measured at 820 nm in pea leaves infiltrated either with DCMU, MV, DCMU+MV or DBMIB.

Table 1
Decay times (τ) of the re-reduction phases of PC^+ and $P700^+$ in darkness after a far-red pre-illumination derived from 820-nm transmission changes

	Fast phase (ms)	Medium phase (s)	Slow phase (s)
Control	89±19	1.03±0.05	7.49±0.42
DCMU	–	2.15±0.06	6.98±0.21
DBMIB	–	4.37±0.07[a]	–
DBMIB+DCMU	–	4.58±0.18	–
MV	66±13	2.96±0.32	16.93±1.23
MV+DCMU	–	–	10.89±0.55

Each individual measurement consists of the average of three to four repetitions on the same leaf; the number of independent experiments was four to eight and each value is given with its standard error.

[a] This value was very sensitive to final concentration DBMIB accumulated in the leaf, which could be manipulated by varying the incubation time with DBMIB (cf. Fig. 6B).

4. Discussion

4.1. Explanations for the IP phase

From the list presented in the introduction it is clear that there is a large number of explanations for the IP phase available in the literature [5–17]. Our results strongly support the oldest theory [5–8] that supposes that a transient block at the acceptor side of PSI and a traffic jam of electrons transiently formed in the electron transport chain are responsible for the IP-induction phase. On the basis of our results and literature data, we provide several arguments against the other interpretations:

(1) In the presence of DBMIB, no IP phase is observed, but the maximum fluorescence level is not affected. This despite the fact that in its presence the maximum fluorescence level coincides with a complete oxidation of P700. In other words, the F_m level is unrelated to the redox state of P700 and this makes variable PSI fluorescence as an explanation unlikely.

(2) It has been observed that the IP phase parallels the reduction of PC^+ and $P700^+$ (after an initial oxidation) [13,27]. Schreiber et al. [13] also showed that the reduction of the PQ pool paralleled the JI phase. On the basis of the known rate constants (e.g., an exchange of a reduced Q_B molecule for an oxidized PQ molecule with a halftime of 1–2 ms [30,31] and a reoxidation of PQH_2, initially, with a halftime of 20 ms, e.g., Refs. [32–34]), one would expect a filling up of the PQ pool in the 2–30-ms time range instead of a reduction of the PQ pool in the 30–200-ms time range. (The exception, in this respect, is a titration with DCMU, where a strong slowdown of the reduction of the PQ pool is induced as the inhibition becomes more severe.) In addition, under in vivo conditions (passive infiltration of non-detached leaves with DCMU in complete darkness), a DCMU treatment does not affect the F_m level (S.Z. Tóth, G. Schansker and R.J. Strasser, submitted to Photosynth. Res.). In other words, PQ pool quenching as an explanation for the IP phase is not supported by the experimental data.

(3) An electric field effect to explain the IP phase [15] is also not supported by our data. MV suppresses the IP phase despite the fact that it allows a continuous electron flow as evidenced by the nearly full oxidation of P700 and PC during the illumination with high intensity red light. On the other hand, in the presence of DBMIB, the number of available electron acceptors, and thus the number of stable charge separations that can occur, is limited, but the F_m is not affected. It can also be noted that the membrane potential peaks around the I level and declines beyond that point (e.g., Ref. [35]).

(4) Given the close correlation between the properties of the IP phase and the electron transport flux beyond the cyt b_6/f complex, an assignment of the IP phase to a separate population of slow PSII reaction centers in the stroma lamellae seems also not very likely. The fact that the relative amplitude of the IP phase depends on the light intensity (Fig. 1, Ref. [15]), being relatively larger at lower light intensities, suggests that the IP phase represents the last and slowest rate-limiting step of the photosynthetic electron transport chain.

(5) The energy redistribution (between PSII and PSI) theory presented by Schreiber and Vidaver [9] had probably to do with the experimental protocol. In dark-adapted anaerobic samples, the PQ pool is reduced and Q_A and the acceptor side of PSI are oxidized (e.g., Refs. [5,6]). In the presence of a reduced PQ pool, Q_A becomes quickly reduced by light. Further excitation of the antenna of PSII is then without effect. At the same time, charge separations in PSI start to create an oxidation of the donor side of PSI, which in turn leads to a transfer of electrons from the PQ pool. However, once the acceptor side of PSI has become reduced, further excitation of the PSI antenna is without effect. The partial oxidation of the PQ pool allows some reoxidation of Q_A and, as a consequence, excitation of the PSII antennae leads again to some stable charge separations. Thus, the special redox properties of the samples gave the impression that there could be an energy redistribution from the antennae of the PSII reaction centers to the antennae of the PSI reaction centers and back.

4.2. MV selectively affects the IP phase

Neubauer and Schreiber [11] concluded that in the presence of MV, at low light intensities the I_1–P (=JP) phase is suppressed and at saturating light intensity specifically the I_2–P (=IP) phase. This would seem to contradict the data presented in Fig. 1. However, the discrepancy may be explained by the fact that, at lower light intensities, the J level disappears as the excitation rate drops below the J level limitation. This has two consequences: (1) The accumulation of Q_A^- occurs only when an even slower bottleneck is reached (in this case the reoxidation of PQH_2); and (2) the IP phase as a fraction of F_v increases in size (cf. Ref. [36]). As a consequence, as the light intensity (=excitation rate) is decreased, accumulation of Q_A^- occurs more and more during the IP phase, representing the slowest process during the first few hundred milliseconds of induction.

4.3. IP phase in thylakoid membranes

In thylakoid membranes the Chl *a* fluorescence induction curve shows two clear phases: OJ and JP. The I-step is not clearly distinguishable or absent [18–21]. This is understandable because during the isolation procedure the ferredoxin on the acceptor side of PSI is washed away. Bukhov et al. [21] have demonstrated that by creating a new pool of electron acceptors beyond the cyt b_6/f complex (in their case by adding TMPD; for the working mechanism of TMPD, see Refs. [33,37]), it is possible to observe a kinetic phase analogous to the IP phase in thylakoid membranes. In leaves we were able to do the inverse and create a thylakoid-like situation using DBMIB or MV.

4.4. DBMIB effects

To show that the effects of DBMIB and MV on the Chl *a* fluorescence induction curve are caused by a block at the cyt b_6/f complex and the accepting of electrons at the acceptor side of PSI, respectively, and not by other unknown side effects, we have thoroughly characterized the effects of these substances on the functional properties of the thylakoid membrane under in vivo conditions.

As shown in Fig. 1A, under our conditions, DBMIB treatment had no effect on the F_m level and very little effect on the F_o level (~4% of F_o). These observations are similar to those made for chloroplasts where it was observed that low concentrations of DBMIB did not affect F_m or F_o [38]. Since oxidized DBMIB is a strong static quencher of fluorescence [39,40], this indicates that the DBMIB

concentrations that accumulated in the thylakoid membranes (with the exception of Fig. 6) are relatively low. Fluorescence induction curves of DBMIB-treated leaves show a slightly higher J level (Fig. 1A). Increasing the effective DBMIB concentration in the leaf by prolonging the incubation time causes a further increase of the J level (Fig. 6C). Though DBMIB can bind to the Q_B site and accept electrons from Q_A, it is a much less effective acceptor than the natural occurring quinone [38,41]. By slowing down the electron transfer reactions at the acceptor side of PSII, DBMIB may seem to mimic the effect of DCMU during the first few milliseconds of a red light pulse. Beyond that point, even slower reactions will mask this effect of DBMIB. The double pulse experiments in Fig. 2 show that during the reoxidation of the electron transport chain in the presence of DBMIB, no dip is observed (cf. Fig. 2A and B). Since DBMIB blocks electron transfer to PSI, this observation supports the theory that the dip depends on PSI activity [5–7] following a mechanism as described at the end of Section 4.1.

4.5. DBMIB as an electron shuttle

The O level of a fluorescence transient measured after a pre-illumination (Figs. 2 and 3) probes the redox state of Q_A at the start of the measuring pulse. After a red pre-pulse, the whole electron transport chain is reduced and quick reoxidation of Q_A^- can only occur via recombination with the donor side of PSII. However, this is only possible if the donor side is in the S_2 or S_3 state. Therefore, the slow phase (τ~40 s in Fig. 3A) in the dark-adaptation kinetics of the O level [42,43] after a pre-pulse may represent the reoxidation of Q_A^- in reaction centers that are in the S_0 or S_1 state. These Q_A^- molecules depend for their reoxidation on an, at least partial, reoxidation of the PQ pool. This is supported by the observation of Bukhov et al. [42] that the slow phase of the recovery of the initial fluorescence level depends on the redox state of the PQ pool. In the presence of DBMIB, the amplitude of the slow phase is much smaller (Fig. 3A). Instead, a phase with a τ~4.3 s is found, indicating that a considerable part of the slowly reoxidizing Q_A^- molecules have found alternative electron acceptors. A similar phenomenon is observed for the dark-adaptation kinetics of the J level (Fig. 3B). In control leaves the J level does not change for the first 10 s after a saturating red pulse. In the presence of DBMIB a faster phase is observed, indicating that a part of the PQ pool reoxidizes faster in the presence of DBMIB. The re-reduction kinetics of PC and P700 after a far-red pre-pulse are relatively fast (τ~4.3 s) despite a block at the cyt b_6/f complex and can be further accelerated by increasing the DBMIB concentration in the leaf (Fig. 6B). All these observations seem to indicate that DBMIB, an artificial quinone that is far less hydrophobic than the naturally occurring one, can bypass the cyt b_6/f complex and donate electrons directly to PC^+ and $P700^+$. Subsequently, the reoxidized DBMIB molecules can migrate to the Q_B site and accept electrons from the Q_A^- molecules that cannot recombine with the donor side of PSII. Support for this interpretation can be found in the literature [29,44]. Farineau et al. [29] observed that DBMIB restored the fast and medium kinetic phases: 10 and 200 μs of the re-reduction of $P700^+$ with a halftime of 10–15 s. This is considerably slower than the 4.3-s decay time we observe here but this difference could be due to the DCMU present in the experiments of Farineau et al. Non-photochemical reduction of PQ (see control transient in Fig. 7) may explain why the presence of DCMU had little effect on the re-reduction kinetics of PC^+ and $P700^+$ in leaves (Fig. 6B). On the other hand, we do observe that a build-up of the DBMIB concentration in the leaf, by increasing the incubation time of the leaves with DBMIB, accelerates the re-reduction kinetics of PC^+ and $P700^+$ (Fig. 6B).

4.6. Re-reduction kinetics of PC^+ and $P700^+$

After a far-red pulse, both PC and P700 are in the oxidized state. In an earlier paper [27], we suggested that PC^+ and $P700^+$ can be re-reduced by either electrons flowing from the stroma via the PQ pool to PC and P700 (slow and medium phases, respectively) or by recombination between the FeS clusters of PSI and $P700^+$ (fast phase). DBMIB which blocks the cyt b_6/f complex has the potential to interfere with a re-reduction path via the PQ pool and MV might affect the recombination reaction by interfering with the acceptor side of PSI.

In leaves that are either fully or nearly completely inhibited by DBMIB the fast re-reduction phase observed in untreated leaves is missing. If the fast phase represents a recombination reaction between the FeS clusters of PSI and $P700^+$ as suggested by us [27], this effect of DBMIB is somewhat unexpected. It is possible to find an explanation of this effect of DBMIB by answering the question why such a recombination reaction can be observed in leaves. During a 10–15-s FR pulse all electrons are taken out of the system and one would expect that the final result would be a completely oxidized acceptor side of PSI. The fact that the amplitude of the fast re-reduction phase becomes smaller as the FR pulse length increases [27] supports this. The fast phase does not disappear completely and this may have to do with a small flux of electrons provided by the stroma or even PSII to the PQ pool. DBMIB does interfere with this electron flow.

4.7. MV and cyclic PSI electron transport

MV is thought to be a very effective electron acceptor that competes strongly with ferredoxin for electrons from the FeS clusters of PSI and, as a consequence, strongly suppresses cyclic electron transfer around PSI [45,46]. Bukhov et al. [47] observed that MV eliminated the

acceleration of the re-reduction of PC^+ and $P700^+$ in heat-treated leaves. The interference of MV with the influx of electrons from the stroma into the PQ pool can also be observed in Fig. 7: no transient re-reduction phase is observed. The lack of electrons flowing from the stroma into the PQ pool also explains why the re-reduction of PC^+ and $P700^+$ is a slow process (see Fig. 6 and Table 1). Also in the presence of DBMIB the oxidation kinetics miss a transient re-reduction phase. Therefore, re-reduction of PC^+ and $P700^+$ by electrons that flow from the stroma through the PQ pool seems to be critical for the observation of a transient re-reduction phase. Assuming that DCMU has no major side effects, the modification of the oxidation kinetics in the presence of DCMU seems to indicate that PSII may play a role in this process too. Although far-red induced excitation of PSII is very limited, it may be just enough to partially compensate for electron loss from the cycle and to maintain cyclic electron transfer around PSI for a few seconds [46].

4.8. Concluding remarks

The data presented here show that for the observation of an IP phase, both an electron flow towards PSI and a transient block at the acceptor side (inactive FNR) are necessary. A block of the electron flow towards PSI by DBMIB as well as the creation of a bypass of the transient block at the acceptor side of PSI by MV result in a disappearance of the IP phase of the Chl *a* fluorescence induction curve. A comparison with data from thylakoid membranes indicates that a third requirement is the presence of an electron acceptor pool with some capacity, be it ferredoxin or TMPD [21], beyond the cyt b_6/f complex.

DBMIB in leaves can bypass its own block at the cyt b_6/f complex and donate electrons directly to PC and P700 at a relatively slow rate (τ~4.3 s). When using DBMIB in leaves, this side effect should be taken into account and high doses (inducing a strong increase of the J level) should be avoided.

We have shown that the IP phase is related to PSI activity and, as mentioned earlier, the JI phase parallels the reduction of the PQ pool [13]. These two observations support the idea that the different steps of the Chl *a* fluorescence induction curve (J, I and P) represent the subsequent kinetic bottlenecks of the electron transport chain. These limitations are the exchange of a reduced PQ molecule at the Q_B site with an oxidized one (J level), the reoxidation of PQH_2 (I level) and the transient block imposed by inactive FNR (P level). There is even some evidence that under certain conditions the amplitude of the IP phase may be a rough indicator of PSI content. For leaves of Mg-deficient sugar beets we observed a (non-linear) relationship between IP phase amplitude and the maximum (reducible/oxidizable) 820-nm transmission amplitude (G. Schansker, C. Hermans and M. Ortega, unpublished data).

Acknowledgements

Financial support by the Swiss National Science Foundation grant no. 3100-057046.99/1 and Federal Office for Education and Science grant no. C990075 is gratefully acknowledged.

References

[1] Govindjee, Sixty-three years since Kautsky: chlorophyll *a* fluorescence, Aust. J. Plant Physiol. 22 (1995) 131–160.
[2] D. Lazar, Chlorophyll *a* fluorescence induction, Biochim. Biophys. Acta 1412 (1999) 1–28.
[3] G. Samson, O. Prasil, B. Yaacoubd, Photochemical and thermal phases of chlorophyll *a* fluorescence, Photosynthetica 37 (1999) 163–182.
[4] R.J. Strasser, M. Tsimilli-Michael, A. Srivastava, Analysis of the chlorophyll a transient, in: G. Papageorgiou, Govindjee (Eds.), Chlorophyll Fluorescence: A Signature of Photosynthesis, Advances in Photosynthesis and Respiration, vol. 19, Kluwer Academic Publishers, The Netherlands, 2004, pp. 321–362.
[5] H. Kautsky, W. Appel, H. Amann, Chlorophyllfluorescenzkurve und Kohlensäureassimilation: XIII. Die fluorescenzkurve und die Photochemie der Pflanze, Biochem. Z. 332 (1960) 277–292.
[6] J.C. Munday, Govindjee, Light-induced changes in the fluorescence yield of chlorophyll *a* in vivo; III. The dip and the peak in the fluorescence transient of *Chlorella pyrenoidosa*, Biophys. J. 9 (1969) 1–21.
[7] U. Schreiber, W. Vidaver, Chlorophyll fluorescence induction in anaerobic *Scenedesmus obliquus*, Biochim. Biophys. Acta 368 (1974) 97–112.
[8] K. Satoh, Fluorescence induction and activity of ferredoxin-$NADP^+$ reductase in *Bryopsis* chloroplasts, Biochim. Biophys. Acta 638 (1981) 327–333.
[9] U. Schreiber, W. Vidaver, The I-D fluorescence transient; an indicator of rapid energy distribution changes in photosynthesis, Biochim. Biophys. Acta 440 (1976) 205–214.
[10] C. Vernotte, A.L. Etienne, J.-M. Briantais, Quenching of the system II chlorophyll fluorescence by the plastoquinone pool, Biochim. Biophys. Acta 545 (1979) 519–527.
[11] C. Neubauer, U. Schreiber, The polyphasic rise of chlorophyll fluorescence upon onset of strong continuous illumination: 1. Saturation characteristics and partial control by the photosystem II acceptor side, Z. Naturforsch. 42c (1987) 1246–1254.
[12] B.-D. Hsu, K.-L. Leu, A possible origin of the middle phase of polyphasic chlorophyll fluorescent transient, Funct. Plant Biol. 30 (2003) 571–576.
[13] U. Schreiber, C. Neubauer, C. Klughammer, Devices and methods for room-temperature fluorescence analysis, Philos. Trans. R. Soc. Lond., B 323 (1989) 241–251.
[14] U. Schreiber, Assessment of maximal fluorescence yield: donor-side dependent quenching and Q_B-quenching, in: O. van Kooten, J.F.H. Snel (Eds.), Plant Spectrofluorometry: Applications and Basic Research, Rozenberg Publishers, Amsterdam, 2002, pp. 23–47.
[15] W.J. Vredenberg, A. Bulychev, Photoelectric effects on chlorophyll fluorescence of photosystem II in vivo. Kinetics in the absence and presence of valinomycin, Bioelectrochemistry 60 (2003) 87–95.
[16] R.J. Strasser, Govindjee, On the O-J-I-P fluorescence transient in leaves and D1 mutants of *Chlamydomonas reinhardtii*, in: N. Murata (Ed.), Research in Photosynthesis, vol. II, Kluwer Academic Publishers, Dordrecht, 1992, pp. 29–32.
[17] U. Schreiber, A. Krieger, Two fundamentally different types of variable chlorophyll fluorescence in vivo, FEBS Lett. 397 (1996) 131–135.

[18] P. Haldimann, R.J. Strasser, Effects of anaerobiosis as probed by the polyphasic chlorophyll *a* fluorescence rise kinetic in pea (*Pisum sativum* L.), Photosynth. Res. 62 (1999) 67–83.
[19] P. Haldimann, M. Tsimilli-Michael, Mercury inhibits the non-photochemical reduction of plastoquinone by exogenous NADPH and NADH: evidence from measurements of the polyphasic chlorophyll *a* fluorescence rise in spinach chloroplasts, Photosynth. Res. 74 (2002) 37–50.
[20] P. Pospisil, H. Dau, Valinomycin sensitivity proves that light-induced thylakoid voltages result in millisecond phase of chlorophyll fluorescence transients, Biochim. Biophys. Acta 1554 (2002) 94–100.
[21] N.G. Bukhov, S. Govindachary, E.A. Egorova, D. Joly, R. Carpentier, *N*,*N*,*N*′,*N*′-Tetramethyl-*p*-phenylenediamine initiates the appearance of a well-resolved I peak in the kinetics of chlorophyll fluorescence rise in isolated thylakoids, Biochim. Biophys. Acta 1607 (2003) 91–96.
[22] A. Trebst, E. Harth, W. Draber, On a new inhibitor of photosynthetic electron-transport in isolated chloroplasts, Z. Naturforsch. 25b (1970) 1157–1159.
[23] H. Böhme, S. Reimer, A. Trebst, The effect of dibromothymoquinone, an antagonist of plastoquinone, on non cyclic and cyclic electron flow systems in isolated chloroplasts, Z. Naturforsch. 26b (1971) 341–352.
[24] P.R. Rich, S.A. Madgwick, D.A. Moss, The interactions of duroquinol, DBMIB and NQNO with the chloroplast cytochrome *bf* complex, Biochim. Biophys. Acta 1058 (1991) 312–328.
[25] J. Harbinson, C.L. Hedley, Changes in P-700 oxidation during the early stages of the induction of photosynthesis, Plant Physiol. 103 (1993) 649–660.
[26] P. Schmidt-Mende, H.T. Witt, Zur plastochinonoxydation bei der Photosynthese, Z. Naturforsch. 23b (1968) 228–235.
[27] G. Schansker, A. Srivastava, Govindjee, R.J. Strasser, Characterization of the 820-nm transmission signal paralleling the chlorophyll *a* fluorescence rise (OJIP) in pea leaves, Funct. Plant Biol. 30 (2003) 785–796.
[28] V. Oja, H. Eichelmann, R.B. Peterson, B. Rasulov, A. Laisk, Deciphering the 820 nm signal: redox state of donor side and quantum yield of Photosystem I in leaves, Photosynth. Res. 78 (2003) 1–15.
[29] J. Farineau, H. Bottin, G. Garab, Effect of dibromothymoquinone (DBMIB) on reduction rates of photosystem I donors in intact chloroplasts, Biochem. Biophys. Res. Commun. 120 (1984) 721–725.
[30] A.R. Crofts, H.H. Robinson, M. Snozzi, Reactions of quinones at catalytic sites; a diffusional role in H-transfer, in: C. Sybesma (Ed.), Advances in Photosynthesis Research, vol. I, Martinus Nijhoff/Dr W Junk Publishers, The Hague, 1984, pp. 461–468.
[31] B.A. Diner, V. Petrouleas, J.J. Wendoloski, The iron–quinone electron acceptor complex of photosystem II, Physiol. Plant. 81 (1991) 423–436.
[32] H.T. Witt, Coupling of quanta, electrons, fields, ions and phosphorylation in the functional membrane of photosynthesis; results by pulse spectroscopic methods, Q. Rev. Biophys. 4 (1971) 365–477.
[33] T. van Voorthuysen, The Electrical Potential as a Gauge of Photosynthetic Performance in Plant Chloroplasts; A Patch Clamp Study, Wageningen Agricultural University, Wageningen, 1997.
[34] D.M. Kramer, C.A. Sacksteder, J.A. Cruz, How acid is the lumen? Photosynth. Res. 60 (1999) 151–163.
[35] P. Joliot, D. Béal, A. Joliot, Cyclic electron flow under saturating excitation of dark-adapted *Arabidopsis* leaves, Biochim. Biophys. Acta 1656 (2004) 166–176.
[36] R.J. Strasser, A. Srivastava, Govindjee, Polyphasic chlorophyll *a* fluorescence transient in plants and cyanobacteria, Photochem. Photobiol. 61 (1995) 32–42.
[37] G. Braun, A.R.J. Driesenaar, E. Shalgi, S. Malkin, Manipulation of the imbalance for linear electron flow activities between photosystems I and II of photosynthesis by cyclic electron flow cofactors, Biochim. Biophys. Acta 1099 (1992) 57–66.
[38] J.M. Bowes, A.R. Crofts, Effect of 2,5-dibromo-3-methyl-6-isopropyl-*p*-benzoquinone on the secondary electron acceptor B of photosystem II, Arch. Biochem. Biophys. 209 (1981) 682–686.
[39] M. Kitajima, W.L. Butler, Quenching of chlorophyll fluorescence and primary photochemistry in chloroplasts by dibromothymoquinone, Biochim. Biophys. Acta 376 (1975) 105–115.
[40] N.G. Bukhov, S. Govindachary, E.A. Egorova, R. Carpentier, Interaction of exogenous quinones with membranes of higher plant chloroplasts: modulation of quinone capacities as photochemical and non-photochemical quenchers of energy in Photosystem II during light–dark transitions, Biochim. Biophys. Acta 1604 (2003) 115–123.
[41] K. Satoh, Y. Kitatani, T. Ichimura, S. Katoh, Interactions between various bezoquinones and the Q_B site of oxygen-evolving photosystem II preparations from the thermophilic cyanobacterium *Synechococcus elongatus*, in: M. Baltscheffsky (Ed.), Current Research in Photosynthesis, vol. I, Kluwer Academic Publishers, Dordrecht, 1990, pp. 583–586.
[42] N.G. Bukhov, P. Mohanty, M.G. Rakhimberdieva, N.V. Karapetyan, Analysis of dark-relaxation kinetics of variable fluorescence in intact leaves, Planta 187 (1992) 122–127.
[43] R.J. Strasser, G. Schansker, A. Srivastava, Govindjee, Simultaneous measurement of photosystem I and photosystem II probed by modulated transmission at 820 nm and by chlorophyll *a* fluorescence in the sub ms to second time range, Proceedings of the 12th International Congress on Photosynthesis, CSIRO Publishing, Melbourne, 2001, S14-003, 6 pp.
[44] R.K. Chain, R. Malkin, On the interaction of 2,5-dibromo-3-methyl-6-isopropylbenzoquinone (DBMIB) with bound electron carriers in spinach chloroplasts, Arch. Biochem. Biophys. 197 (1979) 52–56.
[45] G. Cornic, N.G. Bukhov, C. Wiese, R. Bligny, U. Heber, Flexible coupling between light-dependent electron and vectorial proton transport in illuminated leaves of C3 plants; role of photosystem I-dependent proton pumping, Planta 210 (2000) 468–477.
[46] U. Heber, Irrungen, Wirrungen? The Mehler reaction in relation to cyclic electron transport in C3 plants, Photosynth. Res. 73 (2002) 223–231.
[47] N.G. Bukhov, C. Wiese, S. Neimanis, U. Heber, Heat sensitivity of chloroplasts and leaves: leakage of protons from thylakoids and reversible activation of cyclic electron transport, Photosynth. Res. 59 (1999) 81–93.